

Table 1 Comparison of results

r	λ_0'	p	Square of the fundamental frequency, λ'		
			Eq. (2)	Exact ²	% Error
0.4	4.69	- 0.5	5.61	5.53	- 1.43
		- 1.0	6.52	6.37	- 2.30
		- 2.0	8.33	8.05	- 3.36
		- 10.0	21.85	21.48	- 1.69
0.6	3.57	- 0.5	4.28	4.21	- 1.64
		- 1.0	4.98	4.85	- 2.61
		- 2.0	6.36	6.13	- 3.62
		- 10.0	16.85	16.35	- 2.97
0.8	2.89	- 0.5	3.46	3.41	- 1.45
		- 1.0	4.03	3.92	- 2.73
		- 2.0	5.14	4.96	- 3.50
		- 10.0	13.70	13.24	- 3.36

where

Ω_0', Ω' = square of the fundamental frequency of structure X' at zero axial load and an axial load P , respectively

Ω_0, Ω^* = square of the fundamental frequency of structure X at zero axial load and an axial load P^* , respectively.

The practical implication and use of Eq. (2) are as follows. If we are interested in studying the effect of changes in mass distributions at various levels of axial loads, all that is needed are 1) the fundamental frequencies of a basic mass-distribution case (structure X) at zero and a nonzero axial load, and 2) the fundamental frequency of the mass distribution of interest (structure X') at zero axial load. Generally, a uniform mass distribution may be used as the basic mass-distribution case (structure X). Fundamental frequencies of such structures (beams, plates, shells, etc. with a uniform mass distribution) may be readily available in literature. If the structure is of a more complex nature, these two frequencies may be obtained by analysis or testing.

Numerical Results

Takahashi² presents a series of numerical results for axially loaded cantilever beams with nonuniform mass distributions (uniform mass plus a concentrated mass at the free end). His results are based on the numerical solution of the exact transcendental equation for the fundamental frequency.

The length of the cantilever beam is L , uniform mass is m per unit length, concentrated mass is M , and the axial load is P (compression is positive and tension negative). The fundamental frequency of lateral vibration is ω . The following nondimensional parameters are used: $p = (PL^2/EI)$, $r = (M/mL)$, and $\lambda = (mL^4/EI)\omega^2 = (mL^4/EI)\Omega$. Similarly, λ_0 , λ^* , λ_0' , and λ' are the nondimensional counterparts of Ω_0 , Ω^* , Ω_0' , and Ω' , respectively.

When the mass ratio $r = 0$, we have the uniform mass-distribution case, which will be used as the basic mass-distribution case (structure X). We need two frequencies for this uniform mass-distribution case: one at zero axial load and another at a nonzero axial load; from Ref. 2, we have $\lambda_0 = 12.36$ at $p = 0$ and $\lambda^* = 21.21$ at $p = p^* = 2.0$. The mass distribution is varied by changing the mass ratio r . The square of the nondimensional fundamental frequency (λ_0') for the specific value of r , at zero axial load, is computed by a numerical solution of the frequency equation.

Fundamental frequencies at any nonzero axial load are calculated using Eq. (2); this computation (hand calculation) takes only a few seconds. Frequencies thus computed are compared against Takahashi's exact results² in Table 1. The accuracy of Eq. (2) is extremely good.

The results presented in Table 1 are plotted in Fig. 3. The straight lines represent the approximate solution provided by

Eq. (2). The exact results from Ref. 2 are indicated by dots. All the exact results fall almost on top of or very close to the straight lines.

Concluding Remarks

A simple method of computing fundamental frequencies of axially loaded structures is presented. The excellent accuracy of the method is illustrated by applying it to an axially loaded cantilever beam with nonuniform mass distribution. The method is equally applicable to beams, stiffened or unstiffened plates, and stiffened or unstiffened shells with nonuniform stiffness distributions, complex geometries, and complex boundary conditions.

References

- ¹Sundararajan, C., "Bounds for the Critical Load of Certain Elastic Systems Under Follower Forces," *AIAA Journal*, Vol. 14, No. 5, 1976, pp. 690-692.
- ²Takahashi, K., "Further Results on a Vibrating Beam with a Mass and Spring at the End Subjected to Axial Force," *Journal of Sound and Vibration*, Vol. 84, 1982, pp. 593, 594.

Effect of Transverse Shear Deformation on Imperfection Sensitivity of Cylindrical Panels

Gerald A. Cohen*

Structures Research Associates,
Laguna Beach, California 92652

Introduction

Hui and Du¹ analyzed the initial postbuckling behavior of boron-epoxy antisymmetric cross-ply cylindrical panels under shear loading. The panels are assumed to be long enough to ignore the effect of the boundary conditions at the two curved edges.

For structures with unique symmetrical buckling modes, initial postbuckling and sensitivity to geometric imperfections are essentially determined by Koiter's second postbuckling coefficient b . Briefly, if $b > 0$, the structure can carry postbuckling loads in excess of the critical load, whereas if $b < 0$, the structure is imperfection sensitive and will fail at a load below the critical load.

In Ref. 1, the calculation of the critical load and postbuckling coefficient is based on the Donnell shell theory, and the results are correlated with the curvature parameter

$$\Theta = B/(Rh)^{1/2}$$

where B is the curved panel width, R its radius of curvature, and h its thickness. Within the assumptions of the Donnell theory, the results are independent of the radius-to-thickness ratio R/h .

Cohen and Haftka² reanalyzed the two-layer clamped panels of Ref. 1 using the code FASOR (field analysis of shells of revolution). This analysis, which is based on classical shell theory using a large radius toroidal model with $R/h = 100$ (Fig. 1), predicts imperfection-insensitive panels ($b > 0$) over the range $0 \leq \Theta \leq 8$.

The purpose of this Note is to re-examine these panels considering the effect of radius-to-thickness ratio using both clas-

Received May 9, 1991; revision received July 8, 1991; accepted for publication July 8, 1991. Copyright © 1992 by the American Institute of Aeronautics and Astronautics, Inc. All rights reserved.

*President, P.O. Box 1348.

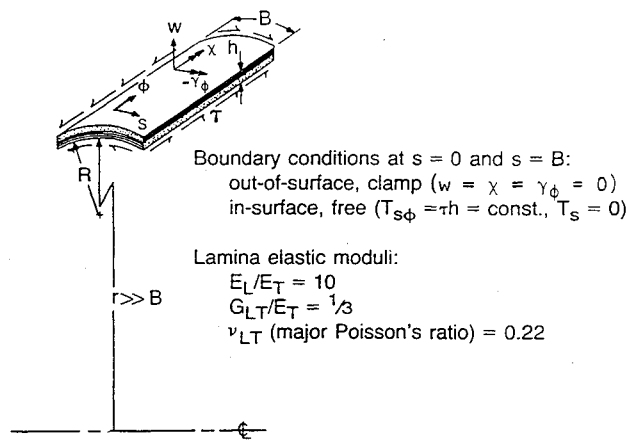
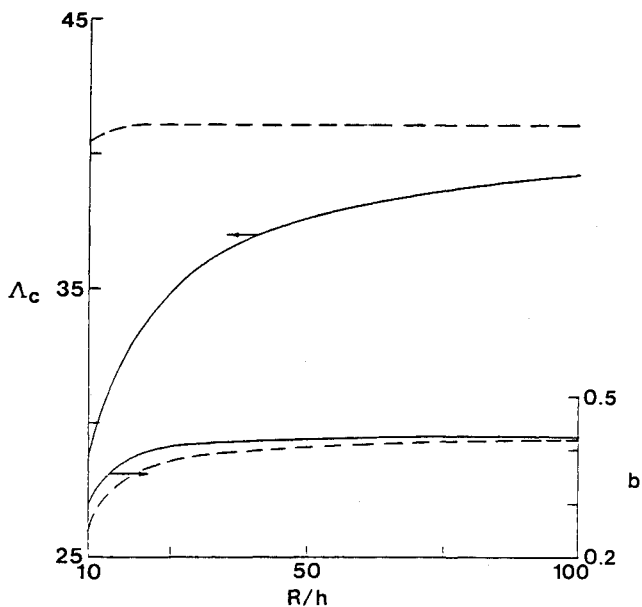
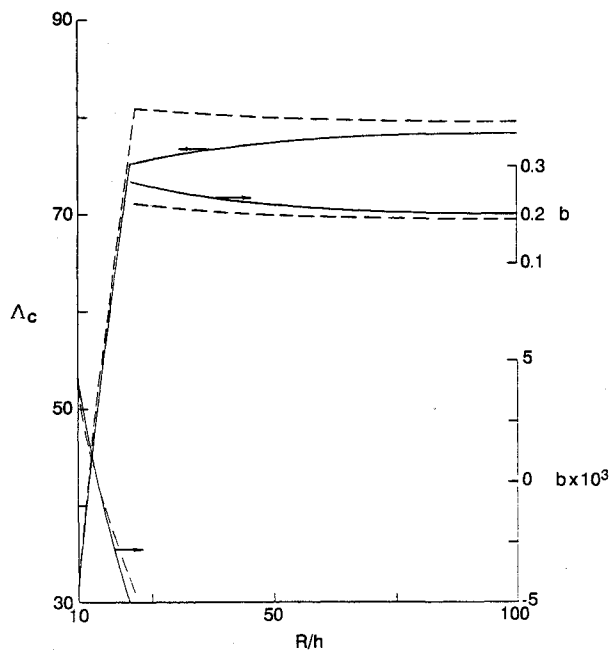


Fig. 1 FASOR model of long two-layer cross-ply cylindrical panel.

Fig. 2 Critical shear stress and postbuckling coefficient of long cross-ply cylindrical panel, $\Theta = 4$.Fig. 3 Critical shear stress and postbuckling coefficient of long cross-ply cylindrical panel, $\Theta = 8$.Table 1 Buckling and initial postbuckling of cross-ply panels, $\Theta = 4^a$

R/h	$l/2B$	Λ_c	b
10	0.779 (0.838)	28.78 (40.42)	0.294 (0.247)
15	0.758 (0.784)	31.80 (40.93)	0.372 (0.332)
25	0.748 (0.761)	34.83 (41.08)	0.406 (0.378)
50	0.743 (0.749)	37.61 (41.08)	0.419 (0.405)
100	0.741 (0.743)	39.22 (41.05)	0.424 (0.419)

^aClassical shell theory results are in parentheses.Table 2 Buckling and initial postbuckling of cross-ply panels, $\Theta = 6^a$

R/h	$l/2B$	Λ_c	b
10	4.503 (4.661)	44.24 (48.17)	-0.0229 (-0.0122)
11	4.592 (4.846)	48.79 (52.83)	-0.0656 (-0.0236)
12	0.611 (5.044)	50.38 (57.26)	0.2886 (-0.0491)
20	0.650 (0.710)	53.24 (59.56)	0.1839 (0.0587)
40	0.682 (0.709)	55.50 (58.73)	0.1283 (0.0810)
100	0.696 (0.708)	56.92 (58.23)	0.1126 (0.0928)

^aClassical shell theory results are in parentheses.Table 3 Buckling and initial postbuckling of cross-ply panels, $\Theta = 8^a$

R/h	$l/2B$	Λ_c	b
10	6.201 (6.114)	30.77 (32.05)	0.00437 (0.00416)
15	6.572 (6.596)	54.15 (55.87)	-0.00084 (-0.00075)
20	7.397 (7.444)	72.79 (74.61)	-0.00471 (-0.00373)
25	0.572 (0.584)	75.71 (80.81)	0.259 (0.219)
50	0.587 (0.594)	77.47 (80.01)	0.221 (0.200)
100	0.595 (0.599)	78.34 (79.61)	0.201 (0.191)

^aClassical shell theory results are in parentheses.

sical shell theory (CST) and transverse shear deformation theory (SDT). As in Ref. 2, the analysis is performed by FASOR using the large radius toroidal model of Fig. 1 with the additional assumption that the transverse shear modulus $G_{TT} = G_{LT}/2$, where L and T signify directions parallel and transverse to the fiber direction of each lamina. Also, the fifth boundary condition on the longitudinal edges of the panel is assumed to be a constraint of the longitudinal transverse shear strain, i.e., $\gamma_\phi = 0$. (Note that the circumferential ϕ direction of the model corresponds to the longitudinal direction of the panel.)

Results

Dimensionless critical shear loads $\Lambda_c (= \tau_c h B^2 / D$, where $D = D_{11} = D_{22}$ is the flexural stiffness of the cross-ply panel), longitudinal buckle wave length l , and postbuckling coefficient b (based on a buckling mode normalization such that its maximum normal deflection equals the panel thickness) from SDT are given in Tables 1–3 for $\Theta = 4, 6$, and 8 , respectively. In these tables, CST results are shown in parentheses. In Figs. 2 and 3, Λ_c and b are plotted for $\Theta = 4$ and 8 , respectively. In these figures, solid lines represent SDT and dashed lines CST.

The following conclusions can be drawn from these results.

1) The Donnell prediction of R/h independence is approximately true for Λ_c (although b has significant dependence on R/h) of CST for R/h greater than a threshold value ρ , which varies from a value less than 10 to 21.5 as Θ varies from 4 to 8. At $R/h = \rho$, the buckling mode abruptly changes from a short wavelength mode to a long wavelength mode, which is highly dependent on R/h . Although the short wave mode is not sensitive to geometric imperfections, the long wave mode is imperfection sensitive, and the sensitivity is greatest for $R/h = \rho$.

2) Aside from the expected result that SDT predicts increasing R/h dependence as R/h diminishes, the SDT results also

display a threshold value of R/h , which is slightly below that for CST (e.g., $\rho = 20.7$ for $\Theta = 8$), to which the previous remarks for CST apply as well. For given values of Θ and R/h , SDT predicts lower critical loads and numerically greater b values than CST. Thus, although the short wave mode is more stable (greater b) than predicted by classical theory, the long wave mode is more imperfection sensitive than predicted by classical theory.

The Koiter buckling load knockdown formula for small imperfections is

$$\Lambda_s/\Lambda_c = 1 + 3(\alpha^2 b \mu^2/4)^{1/2}$$

where Λ_s is the buckling load of the imperfect structure, α an imperfection parameter (unity in this case of pure shear pre-

buckling), and μ the imperfection amplitude-to-thickness ratio. As an example, from Table 2, for $\Theta = 6$ and $R/h = 11$, $b = -0.0656$, giving a knockdown factor of 0.84 for $\mu = 0.1$, or $\Lambda_s = 40.8$. The corresponding value from classical theory is $\Lambda_s = 46.7$.

References

¹Hui, D., and Du, I. H. Y., "Imperfection-Sensitivity of Long Antisymmetric Cross-Ply Cylindrical Panels Under Shear Loads," *Journal of Applied Mechanics*, Vol. 54, June 1987, pp. 292-298.

²Cohen, G. A., and Haftka, R. T., "Sensitivity of Buckling Loads of Anisotropic Shells of Revolution to Geometric Imperfections and Design Changes," *Computers & Structures*, Vol. 31, June 1989, pp. 985-995.

Recommended Reading from Progress in Astronautics and Aeronautics

Space Commercialization: Platforms and Processing

F. Shahrokhi, G. Hazelrigg,
R. Bayuzick, editors

Describes spacecraft that will host commercial ventures, equipment and basic processes that will play major roles (e.g., containerless processing, surface tension, cell separation), and approaches being made in the U.S. and abroad to prepare experiments for space stations. Lessons and guides are included for the small entrepreneur.

1990, 388 pp, illus, Hardback
ISBN 0-930403-76-2
AIAA Members \$59.95
Nonmembers \$86.95
Order #: V-127 (830)

Space Commercialization: Launch Vehicles and Programs

F. Shahrokhi, J.S. Greenberg,
T. Al-Saud, editors

Reviews major launch systems and the development trends in space propulsion, power services of the Space Shuttle, the SP-100 nuclear space power system, and advanced solar power systems. Considers the legal problems developing countries face in gaining access to launch vehicles, presents low-cost satellite and launch-vehicle options for developing countries, and provides business lessons from recent space operational experience.

1990, 388 pp, illus, Hardback
ISBN 0-930403-75-4
AIAA Members \$59.95
Nonmembers \$86.95
Order #: V-126 (830)

Space Commercialization: Satellite Technology

F. Shahrokhi, N. Jasentuliyana,
N. Tarabzouni, editors

Treats specialized communication systems and remote sensing for both host systems and applications. Presents the special problems of developing countries with poor infrastructure, applications of mobile satellite communications, a full range of remote-sensing applications, and Spot Image's case for an international remote-sensing system. Also considered are radiation hazards and solar-energy applications.

1990, 324 pp, illus, Hardback
ISBN 0-930403-77-0
AIAA Members \$59.95
Nonmembers \$86.95
Order #: V-128 (830)

Place your order today! Call 1-800/682-AIAA



American Institute of Aeronautics and Astronautics
Publications Customer Service, 9 Jay Gould Ct., P.O. Box 753, Waldorf, MD 20604
Phone 301/645-5643, Dept. 415, FAX 301/843-0159

Sales Tax: CA residents, 8.25%; DC, 6%. For shipping and handling add \$4.75 for 1-4 books (call for rates for higher quantities). Orders under \$50.00 must be prepaid. Please allow 4 weeks for delivery. Prices are subject to change without notice. Returns will be accepted within 15 days.